

An Introduction to Mössbauer Studies of Magnetic Materials*

S. J. Campbell

Department of Physics, University of New South Wales,
Faculty of Military Studies, Duntroon, A.C.T. 2600.

Abstract

A straightforward introduction to Mössbauer spectroscopy is presented along with a brief background to its discovery over 25 years ago. Several applications of Mössbauer spectroscopy in the study of condensed matter are described. The examples are based on recent investigations of the mixed magnetic *AuFe* system and amorphous alloys and show how Mössbauer spectroscopy can be used to obtain information on local atomic order, magnetic phases and texture. The diverse range of applications of Mössbauer spectroscopy is outlined, including a brief discussion of its use in topics of current interest in metal physics.

1. Introduction to Mössbauer Spectroscopy

(a) Background

The history and rapid development of Mössbauer spectroscopy from its beginnings over 25 years ago as an aspect of research in nuclear resonance fluorescence to its status as a major research tool in the physical and biological sciences is well known (Frauenfelder 1962; Gonser 1975). The painstakingly careful experimental work which led to Mössbauer's (1958*a*, 1958*b*) discovery and theoretical explanation of recoilless nuclear resonance absorption of γ radiation has since served as an inspiration to a generation of Mössbauer spectroscopists.

The impact of Mössbauer's discovery was soon widely acknowledged and appreciated by the scientific community so that only a few years after his graduate studies (1955–8) at the Max Planck Institute in Heidelberg, Mössbauer was awarded the 1961 Nobel Prize for physics at the age of 32. The unusual decision to make such a prestigious award so soon after a discovery is a reflection of the Nobel Prize Committee's view of the fundamental importance of Mössbauer's work. Their assessment of the Mössbauer effect as a widespread research tool for many areas of science has long since been shown to be correct (see e.g. Hanna 1981). No area of physics has benefitted more from Mössbauer spectroscopy than solid state physics.

There are now many books and review articles on the technique; some have been written with a general audience in mind while others have been written from a different perspective with a particular scientific discipline in mind. Indeed, as reported

* Paper presented at the Australia–New Zealand Condensed Matter Physics Meeting, Pakatoa Island, N.Z., 8–10 February 1984.

recently (Stevens *et al.* 1983), Mössbauer spectroscopy is one of the most thoroughly reviewed subjects with over 1200 of the 20 000 Mössbauer publications being review articles. A chronological selection of some of these books and reviews, which cover all of the main areas of application of Mössbauer spectroscopy in both pure and applied science, is given in the Appendix.

Clearly it would not be appropriate to further review the topic; rather, an aim of this paper is to illustrate by examples some of the useful aspects of Mössbauer spectroscopy in the investigation of condensed matter. These examples are based on the ^{57}Fe Mössbauer isotope and are drawn from metal physics, particularly the study of magnetic systems (Section 2). The aim of the general outline to Mössbauer spectroscopy, presented in Section 1*b*, is to introduce the newcomer to the general principles and terms encountered in the subject and to the literature of the field. The continuing development of Mössbauer spectroscopy as a research tool in the study of metal physics is discussed in Section 3 which comprises a list of some of the topics of current interest.

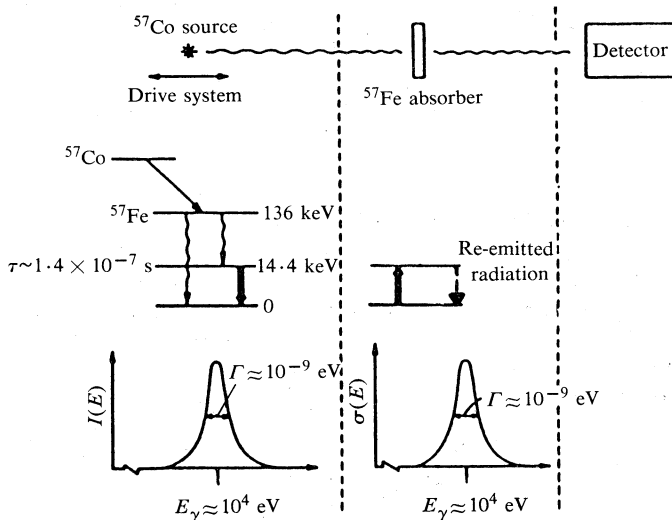


Fig. 1. Schematic representation of a standard Mössbauer transmission apparatus (Gonser 1981*b*). The decay scheme of a ^{57}Co source to ^{57}Fe is also shown with the 14.4 keV Mössbauer transition indicated by the heavy arrows. The high resolution of a Mössbauer experiment can be appreciated from the width of the Lorentzian lineshapes for emission and absorption compared with E_γ , the energy of the transition ($\Gamma/E_\gamma \sim 10^{-9}/10^4 \sim 10^{-13}$).

(b) Experimental Aspects

Mössbauer spectroscopy can be described as nuclear resonance absorption which occurs as a result of the recoil-free emission and recoil-free absorption of γ rays for certain nuclides. This quantum effect arises from zero-phonon transitions in the discrete energy levels for a nucleus bound in a solid (see e.g. Boyle and Hall 1962; O'Connor 1968; Dale 1975; Gonser 1975).

Fig. 1 is a schematic representation of the most common arrangement used in a standard ^{57}Fe Mössbauer transmission experiment. The four main components are the γ -ray source, the absorber, the drive system and the γ -ray detector. Depending

on the particular system under investigation, the first three components may be combined in a number of ways with the most common arrangement being the one depicted in Fig. 1 in which the single-line source vibrates and the absorber is stationary. The term single line is used to describe a source or absorber whose spectral lineshape closely approximates that of the ideal nuclear transition of Lorentzian lineshape. For example, the ^{57}Fe 14.4 keV excited state of mean lifetime $\tau \sim 1.4 \times 10^{-7}$ s corresponds to a Lorentzian line of width $\Gamma_{\text{nat}} \sim 10^{-9}$ eV ($\Gamma\tau = \hbar$) as also depicted in Fig. 1. In practice a combined source and absorber linewidth of $\Gamma_{\text{obs}} = \Gamma_{\text{s}} + \Gamma_{\text{a}} \approx 0.24 \pm 0.02$ mm s $^{-1}$ can be obtained readily in the laboratory compared with the ideal value for the minimum observable linewidth of $2\Gamma_{\text{nat}} = 0.194$ mm s $^{-1}$. The additional broadening is due mainly to thickness effects in samples and to external vibrations.

Table 1. Some topics to be considered in carrying out a Mössbauer transmission experiment

Topic	References
Complete spectrometers	Cranshaw (1974a), Window <i>et al.</i> (1974), Gütlich <i>et al.</i> (1978)
Drive systems	Clark <i>et al.</i> (1967); Cranshaw (1974a)
Calibration	Cranshaw (1974a), Gütlich <i>et al.</i> (1978)
Standard samples; calibration and reference values	Shenoy and Wagner (1978), Stevens <i>et al.</i> (1978–84), Stevens (1983)
Sources	Gol'danskii and Herber (1968), Prowse <i>et al.</i> (1973), Gonser (1975), Gütlich <i>et al.</i> (1978), Stadnik (1978)
Absorber thickness	Margulies and Ehrman (1961), Shimony (1965), Long <i>et al.</i> (1983)
Detectors	Gol'danskii and Herber (1968), Gonser (1975), Gütlich <i>et al.</i> (1978)
Furnaces and cryostats	Gol'danskii and Herber (1968), Gütlich <i>et al.</i> (1978), Herbert <i>et al.</i> (1979)
Mathematical evaluation of spectra; fitting	Muir (1968), Cranshaw (1974b), Gütlich <i>et al.</i> (1978), Keller (1981), Price (1981)

In carrying out a transmission Mössbauer experiment the drive system of Fig. 1 is used to modulate the energy of the γ ray emitted from the single-line source by sweeping the source backwards and forwards, hence supplying a Doppler shift. The sweep velocity range is made large enough to ensure that the energy states of the absorber under investigation are scanned (typically about ± 10 mm s $^{-1}$ for ^{57}Fe investigations). The interactions between the nuclei and their environments lead to changes in the nuclear energy levels resulting in the familiar hyperfine interactions—electric monopole interaction (isomer shift), electric quadrupole interaction and magnetic dipole interaction—which are amenable for study by Mössbauer spectroscopy. When used in this way with a single-line source, the experimentally observed spectrum represents the hyperfine interactions present in the absorber. In the cases of samples which experience just one of the above interactions, the spectra result in a single-line spectrum (electric monopole interaction), a doublet (electric quadrupole interaction) and a six-line spectrum (magnetic dipole interaction) (see e.g. Gonser 1975; Gütlich *et al.* 1978; Berry 1983).

A more detailed discussion of experimental aspects of Mössbauer spectroscopy is beyond the scope of this article. Excellent descriptions of the layout and general

requirements of typical spectrometers are presented by Wertheim (1964), Cranshaw (1974a) and Gütlich *et al.* (1978). Much of the work reported here was carried out using the versatile spectrometer designed and developed by Window *et al.* (1974). Further details about the topics which normally have to be considered in carrying out a Mössbauer experiment can be obtained from the references listed in Table 1.

As well as the transmission mode outlined above, whereby spectra are obtained by counting the γ rays which pass through a resonant absorber, Mössbauer spectra can also be obtained in a scattering geometry. In the scattering technique, the radiation (γ rays, X rays, conversion electrons) which is re-emitted as part of the decay of the excited nuclear state of the sample is detected (see the broken arrow in Fig. 1). Further information on this increasingly important part of Mössbauer spectroscopy, which is used primarily in surface studies, can be obtained from Spijkerman (1971), Champeney (1979) and Sawicka and Sawicki (1981).

Table 2. Some applications of Mössbauer spectroscopy to studies of the properties of metals and compounds

Area	Properties	Area	Properties	Area	Properties
Atomic structure of solids	Phase analysis	Magnetism	Magnetic ordering ^A	Chemistry	Oxidation state
	Atomic arrangements ^A		Phase transition		Electronic configuration
	Site occupancy		Internal fields		Bonding properties
	Diffusion		Spin orientations		
	Solubility limits				
	Precipitation				
	Surface (scattering)				
Texture ^A					

^A Discussed in Section 2.

2. Areas of Application

Although this article is restricted to discussion of the ^{57}Fe Mössbauer isotope, the extent to which Mössbauer spectroscopy lends itself to the study of a wide range of materials is indicated by the Mössbauer periodic table (see Fig. 1.10 of Gonser 1975). Those elements in which the Mössbauer effect has been observed are listed in the table along with the number of isotopes and Mössbauer transitions: over 100 Mössbauer resonances have been observed from 83 isotopes of 44 elements. Of these, the ^{57}Fe and ^{119}Sn isotopes are by far the most commonly used with $\sim 55\%$ and $\sim 12\%$ of published work respectively being devoted to these resonances [the next most commonly used isotope is ^{151}Eu with $\lesssim 2\%$ of the publications (Stevens *et al.* 1983)]. This follows both from the fundamental and technological importance of these elements and the relative ease of carrying out experiments with these resonances. By comparison, the requirements for preparation of sources and absorbers for some of the rare earth isotopes, combined with the need for low temperature environments for both source and absorber in order to increase the recoil-free fraction, can make rare earth Mössbauer experiments quite exacting (see e.g. Prowse *et al.* 1973).

It should also be noted that Mössbauer studies are not just restricted to materials which contain a Mössbauer element. A Mössbauer nuclide can commonly be introduced as a dilute substitutional impurity thus acting as a probe of the sample under investigation [e.g. ^{57}Fe solutes in $\text{NbH}_{0.84}$ and $\text{VD}_{0.78}$ (Wagner *et al.* 1984)]. Care

must then be taken in the interpretation in deciding whether the results apply to the host or to the properties of the host modified by the impurity—particularly for a strongly magnetic impurity such as iron.

Interpretation of hyperfine spectra can yield information on a wide range of topics, including atomic oxidation states, covalency effects, electronegative groups, ligands, site symmetry and the electric field gradient at the nucleus, magnetic ordering as well as the magnitude and direction of the magnetic field at the nucleus. Information can also be obtained from the lineshape (Price 1981) and linewidth behaviour (see e.g. Lauer and Keune 1982) and spectra can also provide information about relaxation effects (see e.g. Dekker 1967; Buckley *et al.* 1970).

Some of the areas of application of Mössbauer spectroscopy to the study of metals and compounds are listed in Table 2, along with an outline of the information which analysis and interpretation of the spectra can provide. This list is by no means complete but merely serves to indicate the diverse areas in which Mössbauer spectroscopy can be applied. A fuller appreciation can be obtained from recent books (Gonser 1975, 1981*a*, 1981*b*) in which the conventional and more exotic applications are described. Three topics in Table 2, atomic arrangements, magnetic ordering and texture, form the basis of the examples described below. These topics are demonstrated by recent studies of the mixed magnetic *AuFe* system and magnetic amorphous alloys.

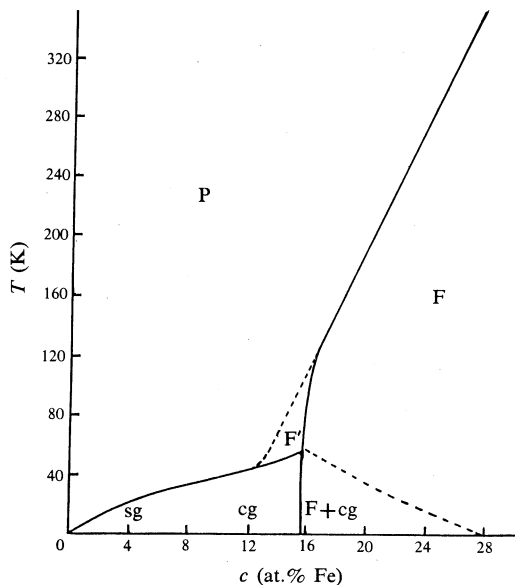


Fig. 2. Magnetic phase diagram of the *AuFe* system: P, paramagnetic; sg, spin glass; cg, cluster glass; F, ferromagnetic; F', quasi-critical region. [Sarkissian (1981).]

(a) Atomic Arrangements

The nature of the magnetic transition to a spin glass state is still unclear, as is the manner in which a spin glass phase merges or coexists with a phase exhibiting long-range magnetic order [for an appraisal of the spin glass transition see Hicks (1983) and Fischer (1983)]. The *AuFe* system is a classic example of such a mixed magnetic system and Fig. 2 shows its magnetic phase diagram. The questions of the double magnetic transitions (paramagnet to ferromagnet and ferromagnet to mixed

magnetic phases) and the co-existence of magnetic phases in the $AuFe$ system are of considerable current interest to both experimentalists (see e.g. Lauer and Keune 1982; Varret *et al.* 1982; Violet and Borg 1983; Beck 1984) and theoreticians (Gabay and Toulouse 1981; Cragg *et al.* 1982; Fischer 1983). A main aim of such studies is to test the predictions and phase diagram of the Heisenberg mean field model in which freezing of only the transverse components of the Heisenberg spins takes place, enabling ferromagnetism and spin glass order to coexist.

Before details of the spin correlations in such a material can be determined it is first necessary to establish the local atomic order. Theories of spin glass behaviour are generally based on random alloy models (Fischer 1983). Whittle and Campbell (1983, 1984) have recently determined the atomic order in a series of $AuFe$ alloys (5, 10, 15 and 20 at. % Fe) by analysing spectra obtained at room temperature—well above their magnetic ordering temperatures (cf. Fig. 2).

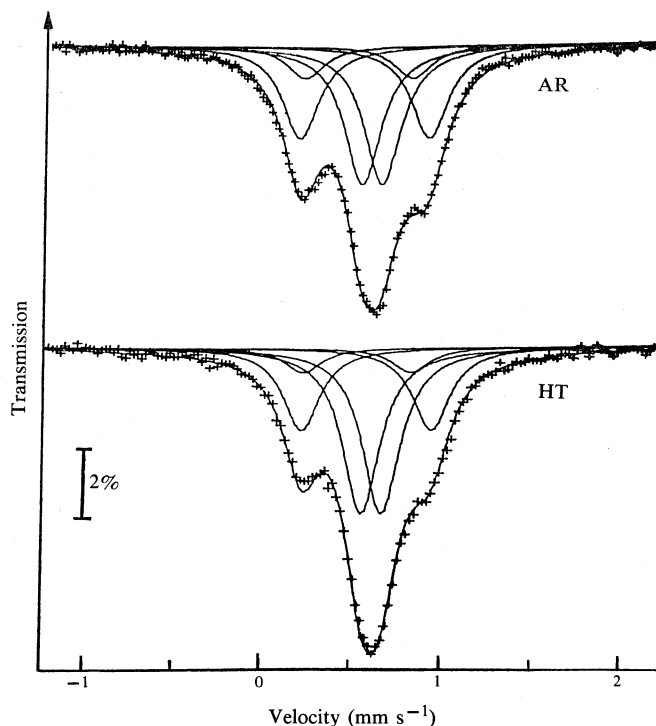


Fig. 3. Room temperature spectra for 5 at. % $AuFe$ alloys in the as-rolled (AR) and heat treated (HT, 550°C for 1 day) states. The subspectra and resultant fits to the spectra are explained in Section 2a. A 2% absorption marker is shown. [Whittle and Campbell (1983).]

Fig. 3 shows the room temperature spectra obtained for the 5 at. % $AuFe$ sample in two different metallurgical states, the as-rolled state (AR) and a heat treated state (HT, 550°C for 1 day). The curves through the data points show the fits to the data based on the subspectra which are also shown. The subspectra, which comprise three doublets of Lorentzian lineshapes, were determined by comparison with a random alloy model calculated using the binomial theorem (Fujita 1975). Details

of the fitting procedure are presented elsewhere (Whittle and Campbell 1983, 1984) but the main result from the spectral analysis is that the fractional areas of the three doublets show slight but significant differences from those expected for a random alloy. These differences can be expressed in terms of the Warren–Cowley atomic order parameter

$$\alpha_1 = (z_1 - c)/(1 - c), \quad (1)$$

where c is the iron concentration and z_1 is the average concentration of iron atoms in the first neighbour shell as determined from the fractional areas of the Mössbauer subspectra (Campbell and Hicks 1975). Fig. 4 shows the α_1 values determined from the spectra using the above analysis for the AuFe alloys in the as-rolled and heat treated states (Whittle and Campbell 1983, 1984). The main conclusion is that the gold and iron atoms are not distributed randomly [i.e. $\alpha_1 = 0$ in equation (1)] as considered by earlier workers but rather that the as-rolled alloys exhibit a tendency for clustering of like atoms ($\alpha_1 > 0$), whereas the heat treated samples show a tendency towards short-range atomic order ($\alpha_1 < 0$) with the unlike atoms clustering together. As considered below, this property is also reflected in the behaviour of the alloys below their magnetic ordering temperatures.

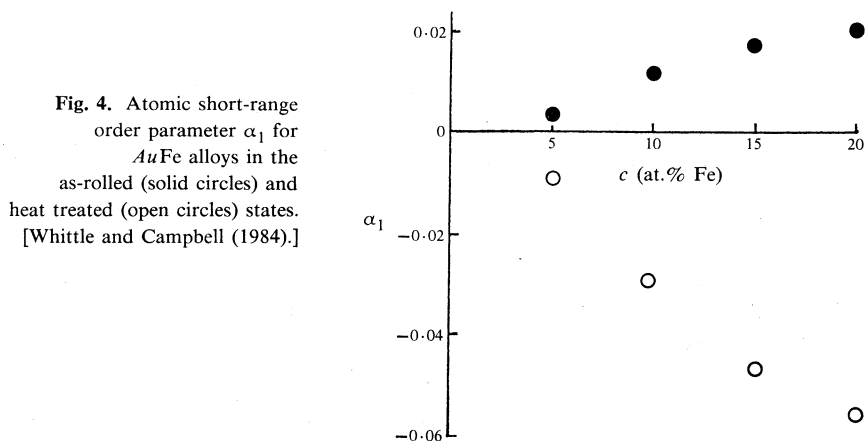


Fig. 4. Atomic short-range order parameter α_1 for AuFe alloys in the as-rolled (solid circles) and heat treated (open circles) states. [Whittle and Campbell (1984).]

(b) Magnetic Properties

Zero field spectra. Fig. 5 shows the 4.2 K spectra for the 10 at.% Fe sample in the AR and HT states. Both spectra show essentially the six-line pattern expected from the nuclear Zeeman effect for a nucleus with a dipole moment which is subject to a magnetic field (see e.g. Gonser 1975). In this case the magnetic field arises from the magnetic hyperfine interaction which occurs below the magnetic transition temperatures of ~ 38 and ~ 41 K for the AR and HT samples respectively (Whittle and Campbell 1984). However, close inspection of the spectra shows that they can be better described in terms of two six-line subspectra which are indicated by the two six-line stick diagrams cg and sg in Fig. 5 (Whittle and Campbell 1983). The significant difference between the AR and HT states is that the fractional area of subspectrum cg has decreased on heat treatment whereas subspectrum sg has increased. These changes are consistent with the mixed cluster glass (cg) and spin glass (sg) magnetic phases obtained by Sarkissian (1981) in this region of the phase diagram

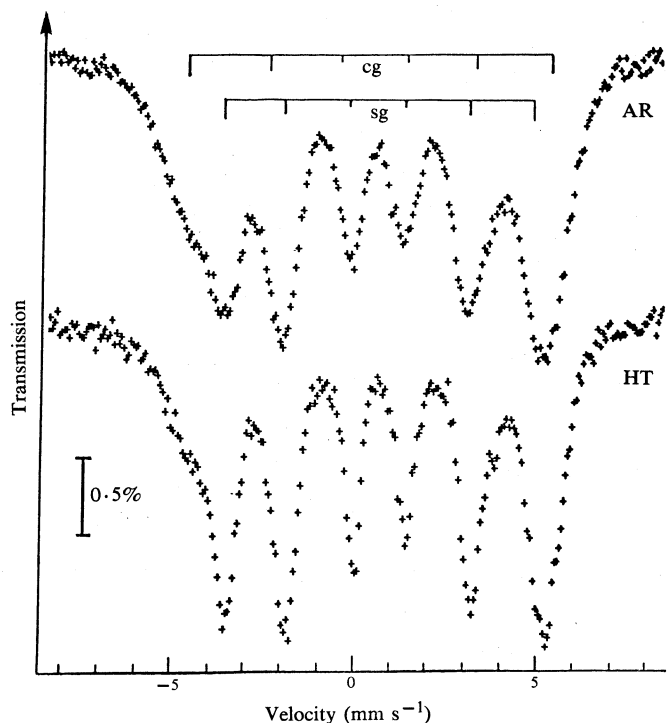


Fig. 5. The 4.2 K spectra for 10 at.% AuFe alloys in the AR and HT states. Both spectra can be well represented by the two six-line subspectra of line positions indicated by the cg and sg stick diagrams. A 0.5% absorption marker is shown. [Whittle and Campbell (1983).]

(Fig. 2). The larger cg component present in the AR sample at low temperatures reflects the atomic clustering and positive α_1 observed in the same sample at high temperatures, well above the influence of magnetic interactions. Similarly the increased area and sharper distribution of the low temperature sg phase in the HT sample indicates a more uniform distribution of spins in the lattice, in agreement with the tendency for atomic short-range order in this sample state. This interpretation is also supported by the applied field spectra presented below.

Applied field spectra. The intensity ratios of the six lines in a magnetically split spectrum depend on θ , the angle between the γ -ray direction and the direction of the magnetic field at the nucleus, in the following manner:

$$I_{1,6} : I_{2,5} : I_{3,4} = 3 : b : 1, \quad (2a)$$

where

$$b = 4 \sin^2 \theta / (1 + \cos^2 \theta). \quad (2b)$$

These relationships afford a useful means of differentiating between magnetic phases. The AuFe phase diagram of Fig. 2 indicates an established ferromagnetic region above a critical percolation limit $c_p \sim 15.7$ at.% Fe with a glass-like phase extending under the ferromagnetic phase. Applied spectra have been used by Whittle *et al.* (1983) to examine the behaviour of these two regions of the phase diagram.

Fig. 6 shows the zero and applied field spectra obtained on a 20 at.% AuFe sample at 80 K. The spectra provide unequivocal evidence for ferromagnetic ordering in

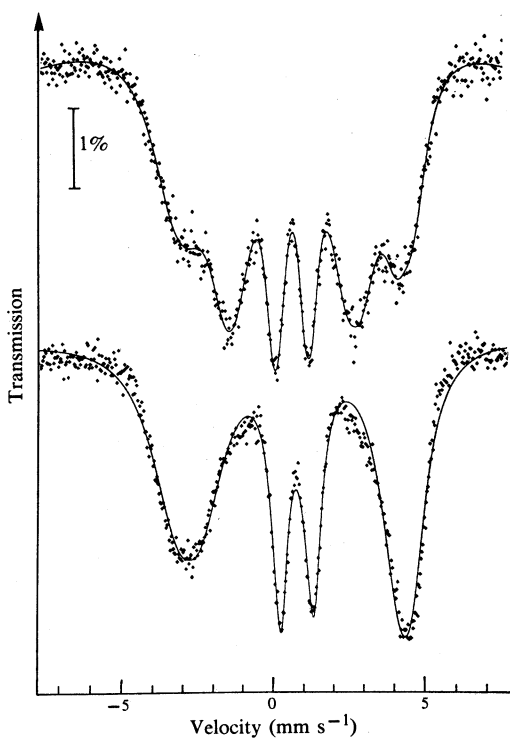
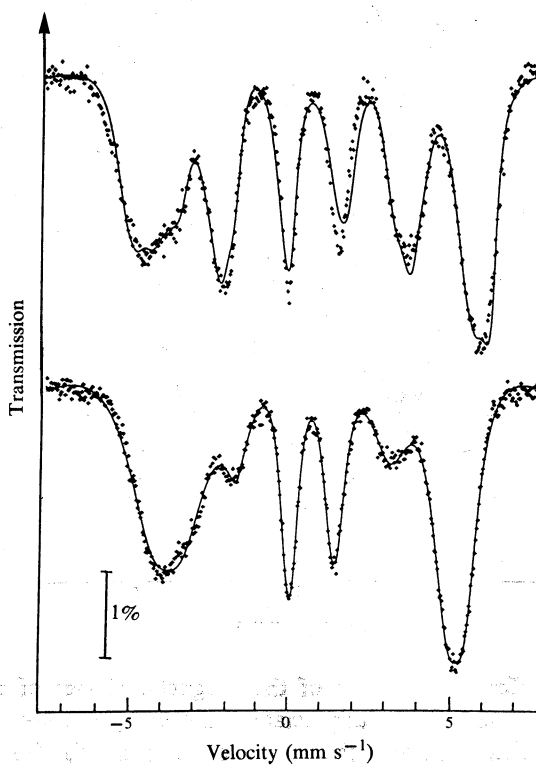


Fig. 6. Zero (upper) and applied (lower) field (5 T) spectra for a 20 at. % AuFe sample at 80 K. A 1% absorption marker is shown.

Fig. 7. Zero (upper) and applied (lower) field (5 T) spectra for a 20 at. % AuFe sample at 4.2 K. A 1% absorption marker is shown. [Whittle *et al.* 1983.]



this region of the phase diagram. The 5 T field was applied in a longitudinal direction parallel to the γ -ray direction and, as expected, the essentially six-line zero field spectrum gives way to a spectrum with four lines in the area ratios 3 : 0 : 1 (equations 2 with $\theta = 0$) on alignment of the magnetic moments with the applied field. This magnetic response at 80 K can be compared with that obtained on the same 20 at. % AuFe sample at 4.2 K (Fig. 7). The zero field spectrum on its own does not permit a statement on the magnetic structure producing the main six lines, but comparison with the 5 T applied spectrum shows that significant changes have taken place in the intensities of the second and fifth lines. The solid curve through the applied field data shows the fit obtained using two six-line subspectra of intensity ratios 3 : 1.6 : 1 and 3 : 0.1 : 1 whereas the zero field data are described by two sextets of intensity ratios 3 : 2.4 : 1 and 3 : 2.6 : 1 (Whittle *et al.* 1983). These results are strong evidence in support of the coexistence of a field responsive ferromagnetic phase and a glass-like phase with frozen magnetic moments which do not respond significantly to the applied magnetic field. The behaviour of the spectra of Figs 6 and 7 is consistent with the merging of the high temperature ferromagnetic phase of AuFe into a combined glass-like and ferromagnetic phase at lower temperatures, in agreement with the phase diagram (see Fig. 2).

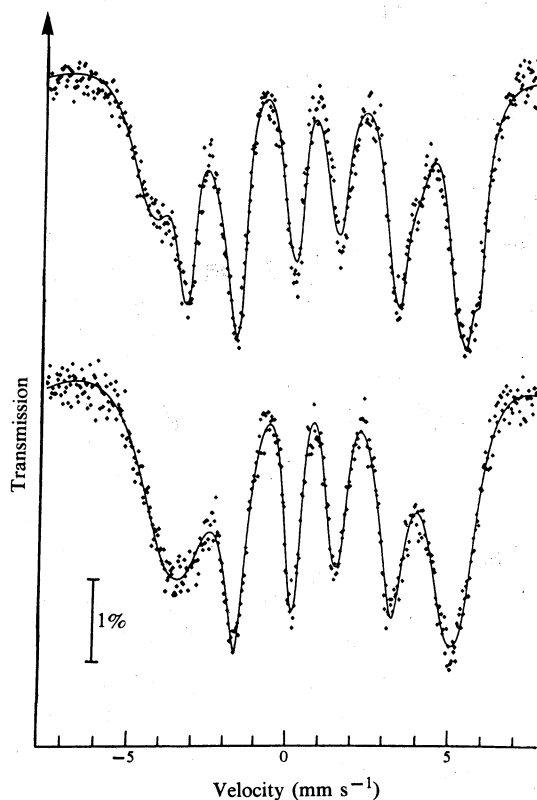


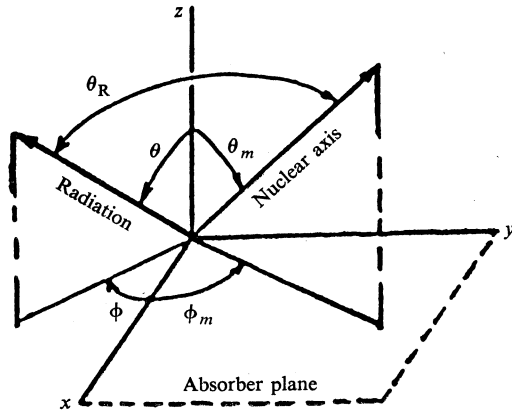
Fig. 8. Zero (upper) and applied (lower) field (5 T) spectra for a 10 at. % AuFe sample at 4.2 K. A 1% absorption marker is shown. [Whittle *et al.* (1983).]

The different responses of the magnetic phases of the AuFe system to applied magnetic fields can be appreciated further by the spectra in Fig. 8. Here there is relatively little change to the zero field spectrum of a 10 at. % AuFe sample at 4.2 K on

application of a 5 T field. This reflects the glass-like nature of this phase with its distribution of frozen moments.

As demonstrated by the above discussion, identification of the magnetic phases from the Mössbauer spectra of a complicated magnetic system such as *AuFe* can be carried out although zero and applied field spectra and detailed spectral analysis are required. Clearly a complex phased iagram such as that of Fig. 2 could be derived by Mössbauer spectroscopy following a complete mapping of temperature and concentration (see e.g. Brand *et al.* 1983). It should be noted, however, that relatively long times ($\sim 10\text{--}50$ h) are usually required to accumulate spectra to the required statistical accuracy in order to determine each point of the phase diagram. In the present example, Mössbauer spectroscopy has been used to examine details of the *AuFe* phase diagram proposed by Sarkissian (1981).

Fig. 9. Axes of the texture problem in Mössbauer spectroscopy; xy is the sample plane, θ and ϕ define the γ -ray direction, θ_m and ϕ_m define the nuclear quantization axis. [Greneche and Varret (1982*a*).]



(c) Texture

Preferred orientations (see e.g. Klug and Alexander 1974) are commonly present in samples as a result of preparation procedures such as cold rolling to produce foils, crystal growth, extrusion of samples, casting, splat-quenching and ribbon spinning. It is clear that anisotropies can be introduced in distributions of assemblies such as crystal grains or magnetic domains; indeed, the textured state is considered to be the most common state for condensed matter (Gonser and Pfannes 1974).

As is clear from the magnetic field polarization effects of the previous subsection, texture or preferred orientation can have a significant influence on spectra. It is therefore important to characterize the state of texture in samples in order to avoid misinterpretation of spectra. Greneche and Varret (1982*a*) have recently developed the established theories of texture in Mössbauer spectroscopy (see e.g. Gonser and Pfannes 1974; Pfannes and Fischer 1977) and used them to obtain either random (i.e. texture-free) spectra or details of the texture distribution, depending on which aspect is more relevant for the particular investigation. The approach taken by Greneche and Varret (1982*a*) in overcoming the problem of texture in Mössbauer spectroscopy is outlined here.

Random spectra. The problem of texture in Mössbauer spectroscopy is represented schematically in Fig. 9 which shows the sample, say absorber, plane xy with the γ -ray direction given by the angles (θ, ϕ) and the nuclear quantization axis defined by (θ_m, ϕ_m) . The unknown texture of the sample can, in the case of axial hyperfine

interactions, be represented by the texture function $\mathcal{D}(\theta_m, \phi_m)$ which describes the number of nuclear quantization axes along the (θ_m, ϕ_m) direction per unit solid angle. The average value $\langle \cos^2 \theta_R \rangle$, where θ_R is the angle between the γ -ray direction and the nuclear quantization axis, is given by (Greneche and Varret 1982a)

$$\langle \cos^2 \theta_R \rangle = \int_0^{2\pi} d\phi_m \int_0^\pi \cos^2 \theta_R \mathcal{D}(\theta_m, \phi_m) \sin \theta_m d\theta_m. \quad (3)$$

This has the value $\langle \cos^2 \theta_R \rangle = \frac{1}{3}$ for the case of a random distribution of nuclear axes. The task of obtaining a random Mössbauer spectrum becomes one of deriving experimental configurations that match the value of $\langle \cos^2 \theta_R \rangle = \frac{1}{3}$. This can be obtained, in the general case of a sample of unknown texture, by superimposing four spectra taken with the sample at the following four orientations:

$$\begin{aligned} \theta^M &= \cos^{-1} \sqrt{\frac{1}{3}}, \text{ any } \phi; & \theta^M, \phi + \frac{1}{2}\pi; \\ \theta^M, \phi + \pi; & & \theta^M, \phi + \frac{3}{2}\pi. \end{aligned}$$

This set of angles is such that the sum of their $\cos^2 \theta_R$ values, determined by equation (3), is (Greneche and Varret 1982a)

$$\sum \cos^2 \theta_R = \frac{4}{3}.$$

The angle $\theta^M = \cos^{-1} \sqrt{\frac{1}{3}} \approx 54^\circ 44'$ is the so-called magic angle, familiar in the magic-angle spinning technique of nuclear magnetic resonance whereby the $3 \cos^2 \theta - 1$ dependent anisotropic interactions present in a sample can be time averaged to zero by high speed spinning at θ^M (Andrew and Wynn 1966). In cases where information is available about the texture in the sample, it is possible to obtain the random spectrum from just one or two judiciously chosen sample orientations.

The ability of this approach to generate random spectra has been amply demonstrated by Greneche and Varret (1982a, 1982b) in their studies of an iron calibration foil and single crystal platelets of RbFeCl_3 .

Population description. In this analysis the opposite approach to that of generating a random spectrum is taken. Here the aim is to obtain quantitative information about any texture that may be present in a sample. This becomes possible with those samples for which the principal axes of texture are known. Such samples might be the cleavage plane of a crystal or the ribbon plane of a melt-spun sample, both of which exhibit mirror symmetry (Greneche and Varret 1982a).

In such a case, with OX, OY and OZ of Fig. 10 representing the principal axes for texture, the populations N_X , N_Y and N_Z along those axes can be determined ($N_X + N_Y + N_Z = 1$). Here the populations, say, in a magnetic sample, correspond to the relative number of spins along each of the principal axes. This population description is not a complete one; rather, it provides a discrete texture which is equivalent to the actual texture present in the sample in the sense that both textures lead to the same angular dependence of $\langle \cos^2 \theta_R \rangle$. The usefulness of this representation stems from the relatively simple expressions which are obtained for $\langle \cos^2 \theta_R \rangle$ when determined with respect to the set of principal axes OX, OY, OZ, for example

$$OX \ (\Theta_m = \frac{1}{2}\pi, \Phi_m = 0), \ \langle \cos^2\theta_R \rangle^{(X)} = N_X \sin^2\Theta \cos^2\Phi, \quad (4a)$$

$$OY \ (\Theta_m = \frac{1}{2}\pi, \Phi_m = \frac{1}{2}\pi), \ \langle \cos^2\theta_R \rangle^{(Y)} = N_Y \sin^2\Theta \sin^2\Phi, \quad (4b)$$

$$OZ \ (\Theta_m = 0, \Phi_m = \frac{1}{2}\pi), \ \langle \cos^2\theta_R \rangle^{(Z)} = N_Z \cos^2\Theta, \quad (4c)$$

where Θ , Φ and Θ_m, Φ_m respectively give the γ -ray direction and nuclear quantization axis with respect to the principal axes and $N_X + N_Y + N_Z = 1$. By carrying out

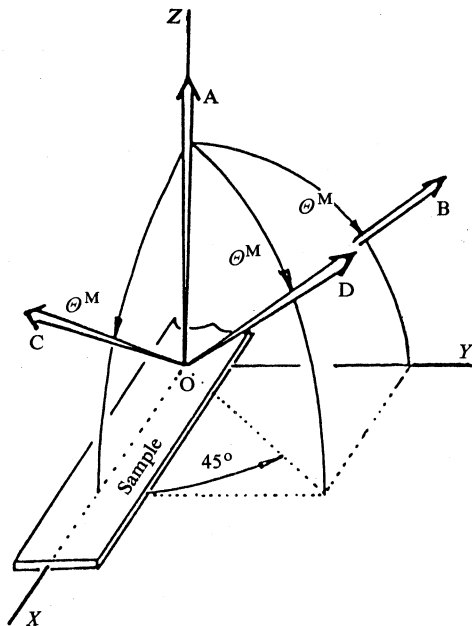
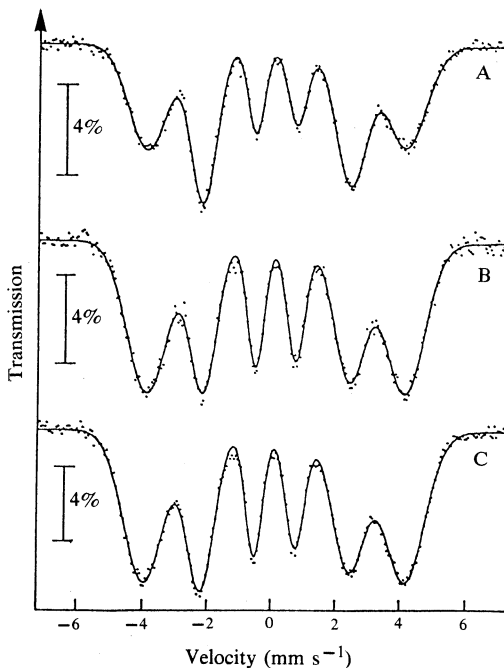


Fig. 10. Four useful orientations A, B, C, D of the γ -ray directions in the principal axes OX, OY, OZ; $\Theta^M = \cos^{-1}\sqrt{1/3} \approx 54^\circ 44'$. [Greneche and Varret (1982a).]

Fig. 11. Room temperature spectra of amorphous ribbon $Fe_{78}Si_{13}B_9$ obtained by using configurations A, B, C of Fig. 10. A 4% absorption marker is shown. [Grün *et al.* (1984).]



Mössbauer experiments at selected values of the angles Θ, Φ , the populations N_X, N_Y and N_Z can be determined. Fig. 10 shows the set of useful orientations proposed by Greneche and Varret (1982a). Configuration D shows that, in the case when the principal axes are known, a random spectrum ($\langle \cos^2 \theta_R \rangle = \frac{1}{3}$) is obtained by directing the γ ray along the (1 1 1) direction.

An example of the usefulness of the population description is given by the spectra in Fig. 11 which were obtained on an amorphous ribbon of $\text{Fe}_{78}\text{Si}_{13}\text{B}_9$ using configurations A, B and C of Fig. 10 (Grün *et al.* 1984). In measuring these spectra the principal axes of texture were taken as (Greneche and Varret 1982a): OX the direction along which the ribbon is spun, OY the width direction and OZ the thickness direction of the ribbon. The solid curves through the spectra show the fits obtained using six gaussian lines and hence, as indicated by equations (2), the average values $\langle \cos^2 \theta \rangle$ can be determined from those measured line intensities; this produces the values $N_X = 0.38$, $N_Y = 0.41$ and $N_Z = 0.14$.* The texture of this sample can therefore be considered to be represented by an ellipsoid of semi-major axes given by these numbers. Grün *et al.* (1984) used this approach to monitor the significant spin reorientation effects caused by the compressive stresses introduced on charging amorphous $\text{Fe}_{78}\text{Si}_{13}\text{B}_9$ with hydrogen.

Table 3. Some topics in metals physics of current interest to Mössbauer spectroscopists

Topics 1, 2 and 3 are closely linked with the strong interest in disordered systems such as spin glasses and amorphous alloys

Topic	Comments
1. Mixed electric and magnetic interactions; overlapped spectra	Validity diagram of Le Caer <i>et al.</i> (1984) acts as a guide to the analysis of such spectra
2. Correlations between hyperfine parameters	Statistical analysis of spectra (Eibschütz and Lines 1982)
3. Radio frequency induced collapse of magnetic hyperfine splitting	Allows electric interactions to be isolated in ferromagnetic amorphous alloys (Kopcewicz <i>et al.</i> 1983)
4. Selective excitation double Mössbauer	Distinguishes between static and dynamic effects; simplifies spectra of distributed static magnetic hyperfine fields
5. Metal hydrogen systems	Gives information on, for example, phases, diffusion and dynamics
6. Energy differential conversion electron Mössbauer spectroscopy	Depth-selective nondestructive analysis of thin films and surface layers (Keune <i>et al.</i> 1983)
7. Texture effects	Important to experimentalists (Greneche and Varret 1982a)

3. Topics of Current Interest

Some of the ways in which Mössbauer spectroscopy contributes to the development of current research interests in metal physics are listed in Table 3. Several of these

* It should be noted that in this example N_X, N_Y and N_Z sum to 0.93 and not the expected 1.0. This indicates that the OX and OY axes are not directed along and perpendicular to the ribbon direction. This slight angle of offset can be determined readily by deriving the polar curve $r(\phi)$ in the sample xy plane and thus determining the exact orientation of the OX and OY axes of the ellipse in this plane.

aspects stem from the strong current interest in disordered systems such as spin glasses and amorphous alloys (see e.g. Chen 1980; Stewart 1983). It is beyond the scope of this article to give other than the following brief outlines of these topics.

The brief comments on the spectra resulting from hyperfine interactions (Section 1*b*) applied to the straightforward cases where just one of the interactions (electric monopole, electric quadrupole or magnetic dipole) is present. The more realistic case of mixed interactions, combined with the complicating effects of distributions of hyperfine parameters resulting in the overlapped spectra commonly encountered in disordered systems, has been analysed fully by Le Caer *et al.* (1984). Their analysis provided a guide as to when standard methods of deconvolution of spectra for distributions of hyperfine fields can be applied (see e.g. Window 1971; Campbell 1983). A related problem is the extent to which correlations exist between hyperfine parameters in amorphous alloys. This has been examined in detail in a series of recent papers by Eibschütz and Lines (e.g. 1982) in which they carry out statistical analyses of spectra in order to derive information on line positions, line widths and mean square fluctuations. This analysis leads to details about the hyperfine field fluctuations and correlations which in turn provides insight into the local atomic environment in amorphous alloys. Comparison with the corresponding correlations in crystalline materials leads to information on the nature of the local structural units (Eibschütz *et al.* 1984).

An experimental approach which will prove useful in studying overlapped spectra is the radio frequency induced collapse method of Kopcewicz *et al.* (1983). Here, for certain amorphous ferromagnets, the magnetization of the sample can be made to follow the reversal of the external r.f. field. This can result in the magnetic hyperfine field at the nuclei being averaged to zero so that only electric interaction effects remain to be detected in a Mössbauer experiment. A further means of simplifying overlapped spectra is by the method of selective excitation double Mössbauer spectroscopy. This technique uses a constant velocity drive to excite particular nuclear energy sublevels and a standard velocity sweep drive to scan the energy of the radiation re-emitted from the scattering sample (Balko and Hoy 1974). Besides enabling dynamic effects such as electronic relaxation (Balko *et al.* 1979) to be distinguished from static magnetic effects, this method can be used to reduce broad distributions of magnetic hyperfine fields to relatively simple spectra comprising perhaps two or three lines (Meisel 1977).

One area in which conventional Mössbauer spectroscopy is playing an increasingly important part is in the investigation of hydrogenated systems, both crystalline (see e.g. Aubertin *et al.* 1984) and amorphous (see e.g. Fries *et al.* 1984). A good example of the diversity of information available from such studies is provided by the recent work of Wagner *et al.* (1984) on iron doped $\text{NbH}_{0.84}$ and $\text{VD}_{0.78}$. Their variable temperature studies (6–400 K) led to information on equilibrium phases, the dynamics of the fluctuating lattice distortions caused by the diffusion of the interstitials and the excitation energies of the hydrogen jump rates.

The combination of ^{57}Fe conversion electron Mössbauer spectroscopy with an electrostatic electron-energy analyser operating under UHV conditions provides a useful technique for depth-selective nondestructive analysis of iron surfaces. The energy differential method is based on the fact that the energy of the conversion electrons which emerge from the surface of the scattering sample, after having experienced inelastic scattering in the solid, is related to their depth of origin below the

surface (Keune *et al.* 1983). This method will prove especially useful for investigating thin film and surface layers.

4. Concluding Remarks

An aim of this article has been to provide a straightforward introduction to Mössbauer spectroscopy to suit the newcomers who will continue to be attracted to the field and those whose main research interests occasionally encounter or overlap Mössbauer spectroscopy. The three applications of Mössbauer spectroscopy presented here have shown the interplay that exists between atomic order and magnetic behaviour in *AuFe* (Whittle and Campbell 1983, 1984), and the spin reorientation effects which take place on charging amorphous ribbons with hydrogen (Grün *et al.* 1984) as monitored using the texture analysis approach of Greneche and Varret (1982*a*).

This article has also sought to emphasize the following main reasons for the continued expansion of Mössbauer spectroscopy as an important tool in condensed matter research:

- (i) Mössbauer experiments are, on the whole, straightforward to carry out. This comment applies mainly to the two resonances in ^{57}Fe and ^{119}Sn , which are the most commonly used isotopes. Exacting demands can, however, be placed on equipment and experimenter by many of the other hundred or so Mössbauer resonances (see e.g. Prowse *et al.* 1973; Deutch *et al.* 1983).
- (ii) Data analysis is also straightforward in many instances although, as topics 1 and 2 of Table 3 suggest, there remain many subtleties and challenges. Once analysis is complete, the interpretation of spectra leads to detailed information.
- (iii) The technique has extensive applications (see Table 2).

This last point is further demonstrated in Section 3 (see Table 3) where some of the wide range of topics of current interest in metal physics were briefly discussed.

Acknowledgments

I thank Dr G. L. Whittle for his careful reading of the manuscript and the two referees of this paper for their helpful suggestions, particularly with regard to the presentation of the material in the first section.

References

- Andrew, E. R., and Wynn, V. T. (1966). *Proc. R. Soc. London A* **291**, 257–66.
- Aubertin, F., Gonser, U., and Campbell, S. J. (1984). Hydride formation by zirconium–iron alloys and the η -phase $\text{Zr}_4\text{Fe}_2\text{O}_{0.6}$. *J. Phys. F* (in press).
- Balko, B., and Hoy, G. R. (1974). In 'Mössbauer Effect Methodology' (Eds I. J. Gruverman, C. W. Seidel and D. K. Dieterly), pp. 307–34 (Plenum: New York).
- Balko, B., Mielczarek, E. V., and Berger, R. L. (1979). *J. Phys. (Paris)* **40**, C2-17–19.
- Beck, P. A. (1984). *J. Appl. Phys.* **55**, 2284–5.
- Berry, F. J. (1983). *Phys. Bull.* **34**, 517–19.
- Boyle, A. J. F., and Hall, H. E. (1962). *Rep. Prog. Phys.* **25**, 441–524.
- Brand, R. A., Manns, V., and Keune, W. (1983). In 'Lecture Notes in Physics', Vol. 192, Heidelberg Colloquium on Spin Glasses (Eds J. L. van Hemmen and I. Morgenstern), pp. 79–89 (Springer: Berlin).
- Buckley, A. N., Herbert, I. R., Rumbold, B. D., Wilson, G. V. H., and Murray, K. S. (1970). *J. Phys. Chem. Solids* **31**, 1423–34.

- Campbell, S. J. (1983). In 'Trends in Mössbauer Spectroscopy' (Eds P. Gütlich and G. M. Kalvius), pp. 117–30 (Univ. of Mainz Press).
- Campbell, S. J., and Hicks, T. J. (1975). *J. Phys.* F 5, 27–35.
- Champeney, D. C. (1979). *Rep. Prog. Phys.* 42, 1017–54.
- Chen, H. S. (1980). *Rep. Prog. Phys.* 43, 353–432.
- Clark, P. E., Nichol, A. W., and Carlow, J. S. (1967). *J. Sci. Instrum.* 44, 1001–4.
- Cragg, D. M., Sherrington, D., and Gabay, M. (1982). *Phys. Rev. Lett.* 49, 158–61.
- Cranshaw, T. E. (1974a). *J. Phys.* E 7, 497–505.
- Cranshaw, T. E. (1974b). *J. Phys.* E 7, 122–4.
- Dale, B. W. (1975). *Contemp. Phys.* 16, 127–46.
- Dekker, A. J. (1967). In 'Hyperfine Interactions' (Eds A. J. Freeman and R. B. Frankel), pp. 679–90 (Academic: New York).
- Deutch, B. I., Kaufmann, E. N., and de Waard, H. (Eds) (1983). *Hyperfine Interactions* 13, 5–236.
- Eibschütz, M., and Lines, M. E. (1982). *Phys. Rev.* B 26, 2288–91.
- Eibschütz, M., Lines, M. E., Chen, H. S., and Masumoto, T. (1984). *J. Phys.* F 14, 505–20.
- Fischer, K. H. (1983). *Phys. Status Solidi (b)* 116, 357–414.
- Frauenfelder, H. (Ed.) (1962). 'The Mössbauer Effect' (Benjamin: New York).
- Fries, S., Wagner, H.-G., Campbell, S. J., Gonser, U., Blaes, N., and Steiner, P. (1984). Hydrogen in amorphous $Zr_{76}F_{24}$. *J. Phys.* F (in press).
- Fujita, F. E. (1975). In 'Mössbauer Spectroscopy' (Ed. U. Gonser), pp. 201–36 (Springer: Berlin).
- Gabay, M., and Toulouse, G. (1981). *Phys. Rev. Lett.* 47, 201–4.
- Gol'danskii, V. I., and Herber, R. H. (Eds) (1968). 'Chemical Application of Mössbauer Spectroscopy' (Academic: New York).
- Gonser, U. (Ed.) (1975). 'Mössbauer Spectroscopy' (Springer: Berlin).
- Gonser, U. (Ed.) (1981a). 'Mössbauer Spectroscopy II' (Springer: Berlin).
- Gonser, U. (1981b). In 'Applications of Nuclear Techniques to the Studies of Amorphous Metals' (Ed. U. Gonser), pp. 203–28 (International Atomic Energy Agency: Vienna).
- Gonser, U., and Pfannes, H.-D. (1974). *J. Phys. (Paris)* 35, C6-113–120.
- Greneche, J. M., and Varret, F. (1982a). *J. Phys.* C 15, 5333–44.
- Greneche, J. M., and Varret, F. (1982b). *J. Phys. Lett. (Paris)* 43, L233–37.
- Grün, J., Blaes, N., Campbell, S. J., Fries, S., Gonser, U., and Wagner, H.-G. (1984). Proc. Int. Meeting on Hydrogen in Metals, Sept. 1983, Poland.
- Gütlich, P., Link, R., and Trautwein, A. (1978). 'Mössbauer Spectroscopy and Transition Metal Chemistry' (Springer: Berlin).
- Hanna, S. S. (1981). In 'Mössbauer Spectroscopy II' (Ed. U. Gonser), p. 189 (Springer: Berlin).
- Herbert, I. R., Timms, K., and Campbell, S. J. (1979). *Cryogenics* 19, 615–17.
- Hicks, T. J. (1983). *Aust. J. Phys.* 36, 519–36.
- Keller, H. (1981). *J. Appl. Phys.* 52, 5268–73.
- Keune, W., Shigematsu, T., Staniék, S., Pfannes, H.-D., Nussbaum, R. H., Brand, R. A., and Saneyoshi, K. (1983). In 'Trends in Mössbauer Spectroscopy' (Eds P. Gütlich and G. M. Kalvius), pp. 27–38 (Univ. of Mainz Press).
- Klug, H. P., and Alexander, L. E. (1974). 'X-ray Diffraction Procedures', pp. 709–54 (Wiely: New York).
- Kopcewicz, M., Wagner, H.-G., and Gonser, U. (1983). *Solid State Commun.* 48, 531–3.
- Lauer, J., and Keune, W. (1982). *Phys. Rev. Lett.* 48, 1850–3.
- Le Caer, G., Dubois, J. M., Fischer, H., Gonser, U., and Wagner, H.-G. (1984). On the validity of ^{57}Fe hyperfine field distribution calculations from Mössbauer spectra of magnetic amorphous alloys (submitted).
- Long, G. J., Cranshaw, T. E., and Longworth, G. (1983). *Mössbauer Effect Ref. Data J.* 6, 42–9.
- Margulies, S., and Ehrman, J. R. (1961). *Nucl. Instrum. Methods* 12, 131–7.
- Meisel, W. (1977). Proc. Int. Conf. on Mössbauer Spectroscopy (Eds D. Barb and D. Jarinä), pp. 71–94 (Central Institute of Physics: Bucharest).
- Mössbauer, R. L. (1958a). *Z. Phys.* 151, 124–43.
- Mössbauer, R. L. (1958b). *Naturwissenschaften* 45, 538–9.
- Muir, A. H., Jr (1968). In 'Mössbauer Effect Methodology', Vol. 4 (Ed. I. J. Gruverman), pp. 75–101 (Plenum: New York).
- O'Connor, D. A. (1968). *Contemp. Phys.* 9, 521–35.

- Pfannes, H. D., and Fischer, H. (1977). *Appl. Phys.* **13**, 317–25.
- Price, D. C. (1981). *Aust. J. Phys.* **34**, 51–6.
- Prowse, D. B., Vas, A., and Cashion, J. D. (1973). *J. Phys. D* **6**, 646–50.
- Sarkissian, B. V. B. (1981). *J. Phys. F* **11**, 2191–208.
- Sawicka, B. D., and Sawicki, J. A. (1981). In 'Mössbauer Spectroscopy II' (Ed. U. Gonser), pp. 139–66 (Springer: Berlin).
- Shenoy, G. K., and Wagner, F. E. (1978). 'Mössbauer Isomer Shifts' (North-Holland: Amsterdam).
- Shimony, U. (1965). *Nucl. Instrum. Methods* **37**, 348–50.
- Spijkerman, J. J. (1971). In 'Mössbauer Effect Methodology', Vol. 7 (Ed. I. J. Gruverman), pp. 85–96 (Plenum: New York).
- Stadnik, Z. M. (1978). *Mössbauer Effect Ref. Data J.* **1**, 217–24.
- Stevens, J. G. (1983). *Hyperfine Interactions* **13**, 221–36.
- Stevens, J. G., Stevens, V. E., and Gettys, W. L. (Eds) (1978–84). *Mössbauer Effect Ref. Data J.*
- Stewart, A. M. (1983). *Met. Forum* **6**, 122–31.
- Varret, F., Hamzić, A., and Campbell, I. A. (1982). *Phys. Rev. B* **26**, 5285–8.
- Violet, C. E., and Borg, R. J. (1983). *Phys. Rev. Lett.* **51**, 1073–6.
- Wagner, F. E., Wordel, R., and Zelger, M. (1984). *J. Phys. F* **14**, 535–47.
- Wertheim, G. K. (1964). 'Mössbauer Effect: Principles and Applications' (Academic: New York).
- Whittle, G. L., and Campbell, S. J. (1983). *J. Magn. Magn. Mat.* **31–34**, 1337–9.
- Whittle, G. L., and Campbell, S. J. (1984). A Mössbauer study of local atomic order in AuFe alloys. *J. Phys. F* (submitted).
- Whittle, G. L., Campbell, S. J., and Maguire, B. (1983). *Hyperfine Interactions* **15/16**, 661–4.
- Window, B. (1971). *J. Phys. E* **4**, 401–2.
- Window, B., Dickson, B. L., Routcliffe, P., and Srivastava, K. K. P. (1974). *J. Phys. E* **7**, 916–21.

Appendix. Bibliography—Chronological Selection of Books and Review Articles

- Lustig, H. (1961). *Am. J. Phys.* **29**, 1–18.
- Boyle, A. J. F., and Hall, H. E. (1962). *Rep. Prog. Phys.* **25**, 441–524.
- Frauenfelder, H. (Ed.) (1962). 'The Mössbauer Effect' (Benjamin: New York).
- Gol'danskii, V. I. (1964). 'The Mössbauer Effect and its Application in Chemistry' (Consultants Bureau: New York).
- Mössbauer, R. L. (1964). 'Nobel Lectures Physics', pp. 584–601 (Elsevier: Amsterdam).
- Wertheim, G. K. (1964). 'Mössbauer Effect: Principles and Applications' (Academic: New York).
- Mössbauer, R. L., and Clauser, M. J. (1967). In 'Hyperfine Interactions' (Eds A. J. Freeman and R. B. Frankel), pp. 497–551 (Academic: New York).
- Gol'danskii, V. I., and Herber, R. H. (Eds) (1968). 'Chemical Application of Mössbauer Spectroscopy' (Academic: New York).
- O'Connor, D. A. (1968). *Contemp. Phys.* **9**, 521–35.
- Greenwood, N. N., and Gibb, T. C. (1971). 'Mössbauer Spectroscopy' (Chapman and Hall: London).
- Bhide, V. G. (1973). 'Mössbauer Effect and its Applications' (Tata McGraw-Hill: New Delhi).
- Bancroft, G. M. (1973). 'Mössbauer Spectroscopy' (McGraw-Hill: London).
- Cranshaw, T. E. (1974). *J. Phys. E* **7**, 497–505.
- Dale, B. W. (1975). *Contemp. Phys.* **16**, 127–46.
- Gonser, U. (Ed.) (1975). 'Mössbauer Spectroscopy' (Springer: Berlin).
- Cohen, R. L. (Ed.) (1976). 'Applications of Mössbauer Spectroscopy I' (Academic: New York).
- Gütlich, P., Link, R., and Trautwein, A. (1978). 'Mössbauer Spectroscopy and Transition Metal Chemistry' (Springer: Berlin).
- Shenoy, G. K., and Wagner, F. E. (1978). 'Mössbauer Isomer Shifts' (North-Holland: Amsterdam).
- Clark, P. E., and Campbell, S. J. (1980). *Met. Forum* **3**, 95–108.
- Cohen, R. L. (Ed.) (1980). 'Applications of Mössbauer Spectroscopy II' (Academic: New York).
- Gonser, U. (Ed.) (1981). 'Mössbauer Spectroscopy II' (Springer: Berlin).

Berry, F. J. (1983). *Phys. Bull.* **34**, 517-19.

Gonser, U., and Preston, R. (1983). In 'Glassy Metals II' (Eds H. Beck and H. J. Güntherodt), pp. 93-126 (Springer: Berlin).

Gütlich, P., and Kalvius, G. M. (Eds) (1983). 'Trends in Mössbauer Spectroscopy' (Univ. of Mainz Press).

Deutch, B. I., Kaufmann, E. N., and de Waard, H. (Eds) (1983). *Hyperfine Interactions* **13**, 5-236. (This special issue of the journal presents 11 review articles to mark the occasion of the 25th anniversary of the Mössbauer effect.)

Manuscript received 22 May, accepted 2 July 1984

